J Solid State Electrochem (2003) 7: 368–373
DOI 10.1007/s10008-002-0329-9

ORIGINAL PAPER

Won-Young Chang · Su-Il Pyun · Seung-Bok Lee

Kinetics of lithium transport through a hard carbon electrode studied by analysis of current transients

Received: 7 May 2002 / Accepted: 11 September 2002 / Published online: 5 February 2003
© Springer-Verlag 2003

Abstract The kinetics of lithium transport through a Carbotron-P hard carbon composite electrode was investigated by analysis of the current transients based upon the modified McNabb-Foster equation. The electrode potential curve ran continuously throughout the whole deintercalation of lithium ions, without the appearance of any potential plateau. However, the anodic current transients showed inflexion points, indicating that several kinds of lithium deintercalation sites present within the electrode are kinetically distinguishable among themselves. Moreover, the anodic current transients did not follow Cottrell behaviour but Ohmic behaviour. The anodic current transients experimentally measured coincided well with those transients numerically simulated based upon the modified McNabb-Foster equation as a governing equation and the "cell-impedance-controlled" constraint as a boundary condition. This strongly indicates that lithium transport is governed by "cell impedance" and at the same time the difference in activation energies for lithium deintercalation between the four different lithium deintercalation sites existing within the electrode accounts for the different kinetics of lithium transport between these sites.

Keywords Hard carbon electrode · Current transient · McNabb-Foster equation · Cell impedance · Numerical simulation

Introduction

For several decades, lithium transport through carbonaceous materials has been usually modelled on the grounds of a "diffusion controlled" concept [1, 2, 3], i.e. slow diffusion of lithium in the electrode, preceded by an extremely fast charge transfer reaction at the interface of electrode and electrolyte. However, in previous work from our laboratory it has been suggested that lithium transport through such transition metal oxides as $Li_{1-\delta}CoO_2$ [4, 5], $Li_{1-\delta}Mn_2O_4$ [6], $Li_{1-\delta}NiO_2$ [5, 7], $Li_{1+\delta}[Ti_{5/3}Li_{1/3}]O_4$ [5, 8] and $Li_\delta V_2O_5$ [5], and a carbonaceous electrode [9, 10, 11], is not limited by lithium diffusion in the bulk electrode but is rather limited by "cell impedance".

It was reported that the disordered carbons, especially hard carbons, showed higher discharge capacities than the theoretical capacity of graphitic materials [12, 13]. These results strongly indicate that lithium ions are intercalated not only into the graphene layers but also into extra sites such as charge transferring surface sites and cluster gaps between the edge planes [12, 13, 14, 15, 16]. Moreover, the potential ranges necessary for lithium intercalation into and deintercalation from the graphene layer and the extra sites are different among themselves, which is caused by the difference in activation energies for lithium intercalation into and deintercalation from the respective sites [16].

This work is aimed at elucidating the mechanism of lithium transport through a Carbotron-P hard carbon composite electrode which contains different kinds of lithium deintercalation sites. For this purpose, open-circuit potential transients and potentiostatic current transients were first experimentally measured. Next, we numerically simulated the anodic current transients based upon the modified McNabb-Foster equation as a governing equation, in combination with the "cell-impedance-controlled" constraint as a boundary condition, to compare with those transients experimentally measured.

Experimental

The electrode specimen used for the working electrode was fabricated from a mixture of as-received Carbotron-P hard carbon powder (Kureha, Japan) and 12 wt% PVDF (polyvinylidene

W.-Y. Chang · S.-I. Pyun (✉) · S.-B. Lee
Department of Materials Science and Engineering,
Korea Advanced Institute of Science and Technology,
373-1 Guseong-Dong, Yuseong-Gu, Daejeon 305-701,
Republic of Korea
E-mail: sipyun@mail.kaist.ac.kr
Tel.: +82-42-8693319
Fax: +82-42-8693310

fluoride) dissolved in NMP (*N*-methylpyrrolidone) solution. The slurry was then pasted on Cu foil and dried at 110 °C for 8 h. A three-electrode electrochemical cell was employed for the electrochemical experiments. Both the reference and counter electrodes were constructed from lithium foil (Foote Mineral, USA; purity 99.9%), and 1 M $LiPF_6$-ethylene carbonate/diethyl carbonate (EC/DEC) (1:1 vol%) was used as the electrolyte.

Galvanostatic intermittent discharge experiments were conducted by using a Solatron 1287 Electrochemical Interface. The discharge current was selected so that a change in lithium content of $\Delta\delta = 1$ for $Li_\delta C_6$ would occur for 5 h. Equilibrium was considered to have been attained when the fluctuation of the open circuit potential fell below 0.1 $mV_{Li/Li+}$. The anodic current transients were measured on the electrode by jumping the initial potentials 0.02, 0.10, 0.20 and 0.40 $V_{Li/Li+}$ to various lithium extraction potentials. Prior to lithium deintercalation, the electrode was maintained at the initial potential for a sufficiently long time to obtain a low steady-state current. In the present work the galvanostatic intermittent discharge curve and potentiostatic current transients were measured on the electrode that had previously undergone at least two cycles of charge-discharge in order to eliminate the effect of the initial irreversible capacity on both the galvanostatic intermittent discharge curve and the current transients. All the electrochemical experiments were performed in a glove box (Mecaplex GB94) filled with purified argon gas.

Results and discussion

Figure 1 presents electrode potentials obtained from the galvanostatic intermittent discharge curve in a 1 M $LiPF_6$-EC/DEC solution as a function of intercalated lithium content. At the same time, the potential ranges necessary for lithium deintercalation from the four different lithium deintercalation sites within hard carbon proposed by Mochida et al. [16] are also given in this figure. The details of the deintercalation potential ranges will be discussed later. The electrode potential curve did not show any "potential plateau"; rather, it ran continuously throughout the whole lithium deintercalation. This means that the Carbotron-P powder has a very low degree of crystallinity, and hence lithium is deintercalated from Carbotron-P particles without formation of any thermodynamically stable phases [9, 10, 11].

Figure 2 illustrates on a logarithmic scale the anodic current transients experimentally measured by jumping the initial electrode potential 0.40 V to various lithium extraction potentials. It should be noted that in order to avoid the double layer discharging effect [17], the initial current levels I_{ini} were measured at 2.5 s, and they were found to be smaller in value by about one order of magnitude than the fictive initial current levels of the corresponding current transients. The fictive initial current level was theoretically determined from the Cottrell equation [18] and its value at the potential jump of 0.40 to 0.42 $V_{Li/Li+}$ is designated in Fig. 2.

Moreover, the current transients did not follow the Cottrell behaviour, which means a linear relationship with a slope of –0.5 on a logarithmic scale, but rather they showed a two-stage current transient behaviour, i.e. a monotonic decrease in logarithmic current with logarithmic time, followed by an exponential decay. The relationship between I_{ini} and potential step, i.e. the difference between the lithium extraction potential E_{ext} and electrode potential E, $\Delta E = |E_{ext} - E|$, in the current transient obeys clearly Ohm's law during the whole

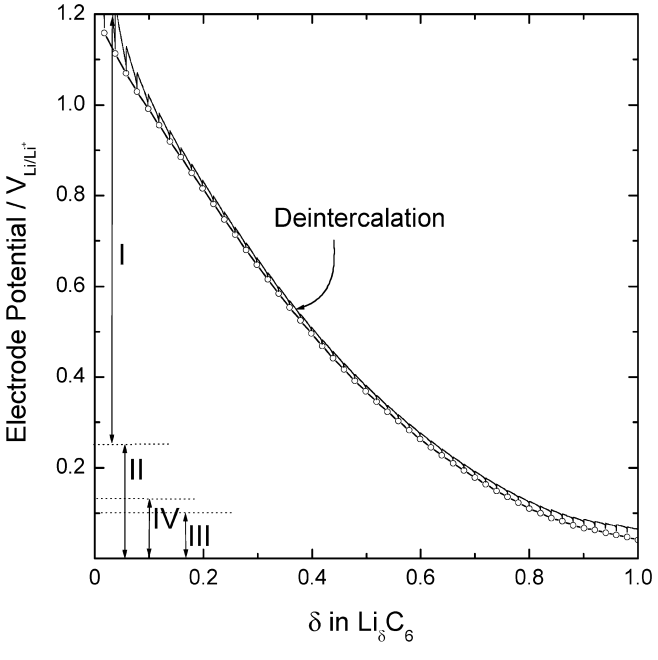

Fig. 1 The galvanostatic intermittent discharge curve measured on the Carbotron-P hard carbon composite electrode in a 1 M $LiPF_6$-EC/DEC solution. Regions I, II, III and IV represent the potential ranges necessary for lithium deintercalation from the sites for type I, type II, type III and type IV, respectively

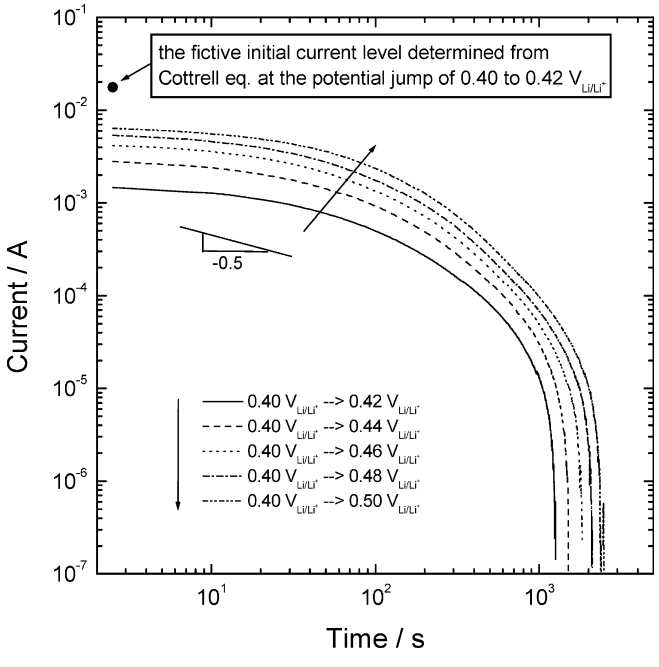

Fig. 2 The anodic current transients experimentally obtained from the Carbotron-P hard carbon composite electrode in a 1 M $LiPF_6$-EC/DEC solution at potential jumps of 0.40 $V_{Li/Li+}$ to various lithium extraction potentials as indicated in figure

lithium deintercalation. In addition, it is noted that the value of the "cell impedance" (15.2 Ω) calculated from the slope of I_{ini} vs. ΔE, coincided well with the internal cell resistance (15.5 Ω) obtained from a.c. impedance spectra measured on the Carbotron-P hard carbon composite electrode.

Similarly, the value of the "cell impedance" calculated from the current transient was in good agreement with that of the internal cell resistance obtained from a.c. impedance spectra measured on the SFG6 graphite composite electrode [9]. Based upon the linear relationship between I_{ini} and ΔE, and the coincidence in value between "cell impedance" and the internal cell resistance, it is strongly suggested that lithium transport through the Carbotron-P hard carbon composite electrode proceeds under the "cell-impedance-controlled" constraint.

Figure 3 envisages on a logarithmic scale the anodic current transients experimentally measured by jumping the initial electrode potential 0.20 V to various lithium extraction potentials. It is noted that the initial current levels I_{ini} experimentally measured at 5.0 s were smaller in value by about one order of magnitude than those fictive initial current levels theoretically determined from the Cottrell equation [18] and one of the theoretical values at the potential jump of 0.20 to 0.24 $V_{Li/Li+}$ is designated in Fig. 3. Moreover, the current transients did not follow Cottrell behaviour. The relationship between I_{ini} and ΔE follows Ohm's law.

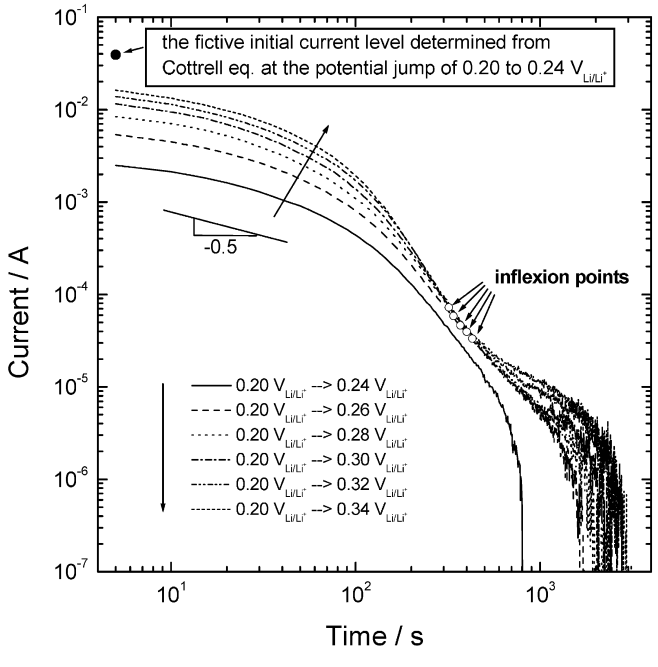

Fig. 3 The anodic current transients experimentally measured on the Carbotron-P hard carbon composite electrode in a 1 M $LiPF_6$-EC/DEC solution by jumping the initial electrode potential 0.20 $V_{Li/Li+}$ to various lithium extraction potentials as indicated in figure

The shape of the current transient measured at the potential jump of 0.20 to 0.24 $V_{Li/Li+}$ was somewhat different from those measured at the potential jumps of 0.20 to various lithium extraction potentials of 0.26 to 0.34 $V_{Li/Li+}$. The former current transient showed two-stage current transient behaviour. By contrast, the latter current transients showed three-stage current transient behaviour, which is characterized by the presence of an inflexion point, i.e. a "quasi-current plateau".

It is well known [4] that under the "cell-impedance-controlled" constraint, the presence of an inflexion point, i.e. a "current plateau" in the current transient, is due to the presence of a "potential plateau" indicating the coexistence of two phases in the electrode potential curve. However, in the case of the Carbotron-P hard carbon composite electrode, the anodic current transients clearly showed an inflexion point, i.e. a "current plateau", even though the electrode potential curve did not show any "potential plateau" throughout the whole lithium deintercalation.

In this work, such abnormal current transient behaviour showing the "inflexion point" at the Carbotron-P hard carbon composite electrode could be reasonably explained in terms of the difference in activation energies for lithium deintercalation. It was reported [16] that there exist four kinds of lithium deintercalation sites within hard carbon, such as a charge transferring surface site, an intercalation site between graphene layers, a cluster gap between edge planes and, finally, a microvoid surrounded by hexagonal planes, which are designated as the sites type I, type II, type III and type IV, respectively. In addition, the potential necessary for lithium deintercalation from the sites for type I, type II, type III and type IV ranges between 0.25 and 2.00 $V_{Li/Li+}$, 0 and 0.25 $V_{Li/Li+}$, 0 and 0.10 $V_{Li/Li+}$ and 0 and 0.13 $V_{Li/Li+}$, respectively.

Remembering the potential range for lithium deintercalation reported by Mochida et al. [16], it is readily realized that lithium ions present in the site for type II can be deintercalated only by the potential jump of 0.20 to 0.24 $V_{Li/Li+}$. In contrast, lithium ions residing in the site for type I as well as the site for type II can be deintercalated just by the potential jumps of 0.20 to the lithium extraction potentials higher than 0.25 $V_{Li/Li+}$. It follows, therefore, that the current transients clearly show simple diffusion behaviour at the lithium extraction potential below 0.25 $V_{Li/Li+}$. By contrast, the current transients exhibit a transition of simple diffusion behaviour to that transient involving an inflexion point, i.e. a "quasi-current plateau" at the lithium extraction potentials above 0.25 $V_{Li/Li+}$.

Now let us theoretically consider lithium transport through the Carbotron-P hard carbon composite electrode. Since lithium transport through the different kinds of lithium deintercalation sites present within hard carbon is conceptually similar to hydrogen transport through the normal sites and the trap sites existing within a metal, the McNabb-Foster equation [19, 20] holds for the case of lithium transport through hard

carbon. In addition, since hard carbon contains three-dimensional diffusion paths and the individual particles are observed to be almost spherical in shape, we selected the constituent particle of spherical symmetry for the theoretical calculation. Thus, in this work, the McNabb-Foster equation was modified to satisfy spherical symmetry and it was used as a governing equation for lithium transport as follows:

$$\tilde{D}_{\mathrm{Li}}\left[\frac{2}{R*}\left(\frac{\partial c}{\partial r}\right)+\frac{\partial^2 c}{\partial r^2}\right]=\frac{\partial c}{\partial t}+N\frac{\partial \theta}{\partial t} \tag{1}$$

with the rate of reversible trapping into and escaping from the trap sites described by:

$$\frac{\partial \theta}{\partial t}=kc(1-\theta)-p\theta \tag{2}$$

where $\tilde{D}_{\mathrm{Li}}$ is the chemical diffusivity of lithium, R^* the average radius of the carbon particle, c the local concentration of lithium, r the distance from the centre of the particle, t the deintercalation time, N the concentration of the trap sites, θ the fraction of the trap sites occupied, k the capture rate into the trap sites, and p represents the release rate from the trap sites. The initial condition (IC) and the boundary conditions (BC) are given as:

$$\mathrm{IC}: \quad c=c_0 \quad \text{for } 0<r<R^* \text{ at } t=0 \tag{3}$$

$$\mathrm{BC}: \quad zFA_{\mathrm{ea}}\tilde{D}_{\mathrm{Li}}\left(\frac{\partial c}{\partial r}\right)=0 \ \text{(impermeable constraint)} \quad \text{for } r=0 \ \ t>0 \tag{4}$$

$$\mathrm{BC}: zFA_{\mathrm{ea}}\tilde{D}_{\mathrm{Li}}\left|\frac{\partial c}{\partial r}\right|=\frac{\Delta E}{R_{\mathrm{cell}}} \ \text{(cell-impedance-controlled constraint) for } r=R^* \text{ at } t>0 \tag{5}$$

where z is the valence number of lithium ion, F the Faraday constant, A_{ea} the electrochemically active area, $\Delta E=|E_{\mathrm{ext}}-E|$ and R_{cell} represents the cell impedance.

In this work, the values of R_{cell} and R^* were estimated to be 15.2 Ω from the current transient and ca. 5 μm from scanning electron microscopy, respectively. $\tilde{D}_{\mathrm{Li}}$ was measured to be 8×10^{-9} $\mathrm{cm^2\ s^{-1}}$ at the electrode potential 0.20 $\mathrm{V_{Li/Li+}}$ by the equation derived by Weppner and Huggins [21] from the galvanostatic intermittent titration curve. Because the amount of Carbotron-P powder in an electrode was 4 mg, A_{ea} was determined to be 13 $\mathrm{cm^2}$, assuming the particle is composed of a perfect sphere.

The capture rate (k) and release rate (p) are defined as the number of lithium jumps per unit time from the lattice site to the trap site, and the jumps per unit time from the trap site to the lattice site, respectively. The capture rate and release rate were determined in the following sequences: first, the chemical diffusivity, $\tilde{D}_{\mathrm{Li}}$, was experimentally determined as a function of the cell temperature from the galvanostatic intermittent titration curve, at the electrode potentials of 0.20 and 0.70 $\mathrm{V_{Li/Li+}}$. The former potential of 0.20 $\mathrm{V_{Li/Li+}}$ is considered as a potential at which lithium ions can be deintercalated only from the site for type II, and the latter potential of 0.70 $\mathrm{V_{Li/Li+}}$ counts as the potential at which lithium ions can be deintercalated only from the site for type I. Next, the activation energy E_{a} for lithium deintercalation from the site for type I and the E_{a} for lithium deintercalation from the site for type II were determined in value to be 85.44 kJ $\mathrm{mol^{-1}}$ (0.89 eV) and 69.70 kJ $\mathrm{mol^{-1}}$ (0.72 eV), respectively, from the Arrhenius plot of $\tilde{D}_{\mathrm{Li}}$, which is given in Fig. 4a.

Finally, since the activation energy for lithium deintercalation from the site for type I is higher in value than the activation energy from the site for type II, we can regard the site for type I as a trap site and the site for type II as a lattice site. In this work, such a trap site as well as a lattice site represent lithium deintercalation sites. Thus, the capture rate and release rate can be obtained from the temperature dependence of three-dimensional random jump by:

$$k=\frac{1}{6}v^*\exp(-69,700/RT)=1.0\ \mathrm{s^{-1}} \tag{6}$$

$$p=\frac{1}{6}v^*\exp(-85,440/RT)=1.7\times10^{-3}\ \mathrm{s^{-1}} \tag{7}$$

where v^* means the maximum vibrational frequency defined by Debye and is usually taken as 10^{13} $\mathrm{s^{-1}}$ for lithium ions [22, 23], R is the gas constant and T is the absolute temperature.

Considering the potential ranges necessary for lithium deintercalation from various sites within hard carbon proposed by Mochida et al. [16], lithium ions present in the site for type II can be deintercalated only by the potential jump of 0.20 to 0.24 $\mathrm{V_{Li/Li+}}$. On the other hand, lithium ions existing in the site for type I as well as the site for type II can be deintercalated just by potential jumps of 0.20 to the lithium extraction potentials above 0.25 $\mathrm{V_{Li/Li+}}$. Thus, we took zero at the lithium extraction potential below 0.25 $\mathrm{V_{Li/Li+}}$ as the initial value of the fraction occupied in the site for type I, θ_{I}. In contrast, we took unity at the lithium extraction potentials above 0.25 $\mathrm{V_{Li/Li+}}$ as the initial value of the fraction occupied in the site for type I, θ_{I}. At the same time, from analysis of the galvanostatic intermittent discharge curve measured on the Carbotron-P hard carbon composite electrode, the concentrations of the trap sites, N, i.e. the amounts of lithium deintercalated from the site for type I, were determined to be 0, 3.9×10^{-4}, 7.9×10^{-4}, 1.2×10^{-3}, 1.6×10^{-3} and 1.9×10^{-3} mol $\mathrm{cm^{-3}}$ at the potential jumps of 0.20 $\mathrm{V_{Li/Li+}}$ to 0.24, 0.26, 0.28, 0.30, 0.32 and 0.34 $\mathrm{V_{Li/Li+}}$, respectively.

Figure 4b illustrates on a logarithmic scale the anodic current transients by jumping the initial electrode potential 0.20 to various lithium extraction potentials (solid lines), determined from the numerical solution to the modified McNabb-Foster equation of Eqs. 1 and 2 with IC and BC of Eqs. 3, 4, 5 by taking the values described above.

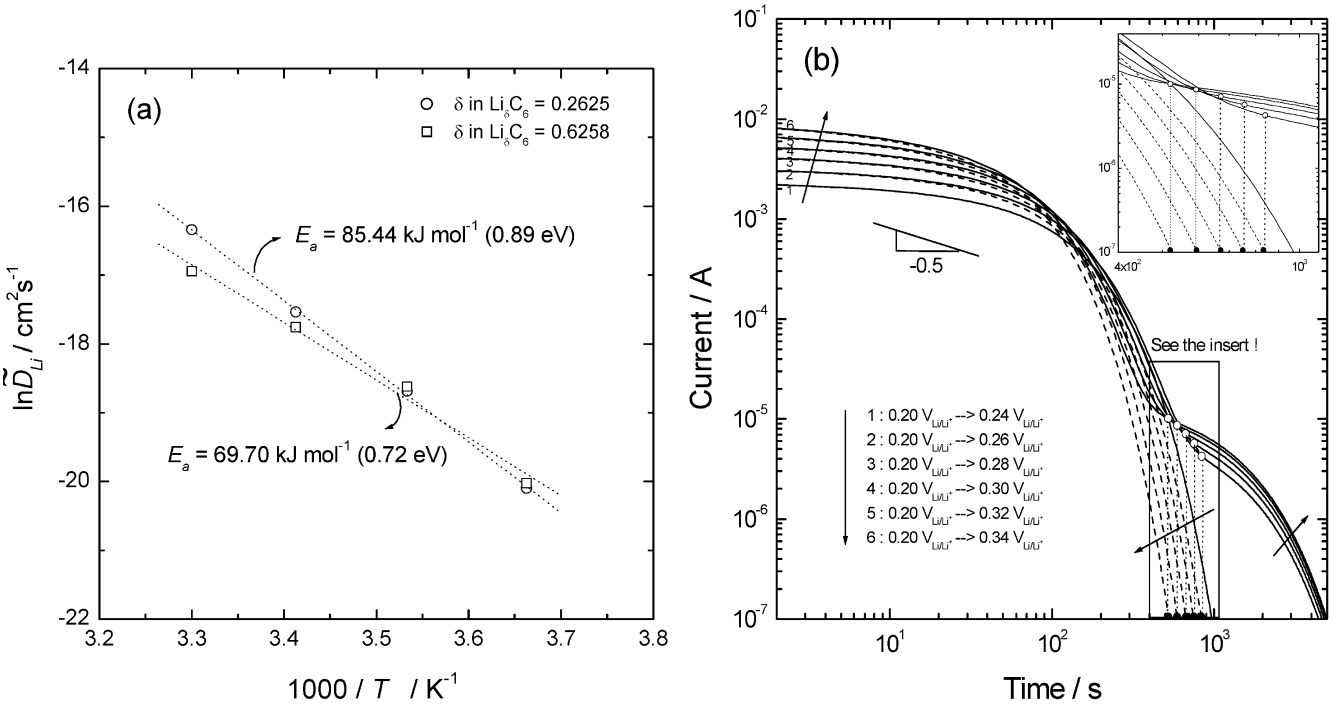

Fig. 4 **a** Arrhenius plots for the chemical diffusivity of lithium in the Carbotron-P hard carbon composite electrode, and **b** the anodic current transients theoretically calculated based upon the modified McNabb-Foster equation (*solid line*) and calculated under the assumption of lithium ion transport through a single phase in the absence of any trap sites (*dashed line*) at potential jumps of 0.20 $V_{Li/Li+}$ to various lithium extraction potentials under the cell-impedance-controlled constraint, by taking $A_{ea} = 13$ cm^2, $tilde D_{Li} = 8\times10^{-9}$ cm^2 s^{-1}, $R_{cell} = 15.2$ Ω and $R^* = 5$ μm

The anodic current transient at the potential jump of 0.20 to 0.24 $V_{Li/Li+}$ showed two-stage current transient behaviour, i.e. a monotonic decrease in logarithmic current with logarithmic time, followed by an exponential decay. However, those current transients at the potential jumps of 0.20 $V_{Li/Li+}$ to the lithium extraction potentials of 0.26 to 0.34 $V_{Li/Li+}$ exhibited an inflexion point, i.e. a "quasi-current plateau".

In addition, in order to clearly specify the physical meaning of the inflexion point, we theoretically simulated the current transients under the assumption of lithium ion transport through a single phase in the absence of any trap sites. They are also presented in Fig. 4b (dashed lines). From Fig. 4b it was realized that the time to complete lithium deintercalation from the site for type II (closed circles), simulated under the assumption of simple diffusion behaviour in the absence of the trap sites, is exactly the same as the time to the inflexion points (open circles) simulated under the assumption of lithium transport in the presence of the trap sites. Thus, in general, the time to the inflexion point in the current transient measured on the electrode in the presence of the trap sites can be regarded as the time to complete lithium deintercalation from the lattice sites with a shallow potential well. This result is consistent with our previous work [10] on soft carbon electrodes.

The anodic current transients theoretically calculated based upon the modified McNabb-Foster equation along with the cell-impedance-controlled constraint of Fig. 4b almost coincided with those current transients experimentally measured in Fig. 3 in value and in shape. This strongly indicates that the appearance of an inflexion point in the current transient is due to lithium deintercalation from two different kinds of deintercalation sites, with clearly distinguishable activation energies.

Until now, we quantitatively analysed the anodic current transients measured on the Carbotron-P hard carbon composite electrode in terms of the difference in activation energies for lithium deintercalation from the different deintercalation sites. However, it is very hard to quantitatively distinguish between deintercalation sites with comparable activation energies for lithium deintercalation. Figure 5a presents the anodic current transients experimentally measured by the potential jumps of 0.10 $V_{Li/Li+}$ to various lithium extraction potentials. All the anodic current transients showed three-stage current transient behaviour, which means they involve one inflexion point throughout the whole lithium deintercalation. At any potential jumps within this potential range, lithium ions occuping both the sites for type II and type IV can be deintercalated. The appearance of the inflexion point in Fig. 5a is due to the difference in activation energies for lithium deintercalation from the site for type II and from the site for type IV.

Figure 5b envisages on a logarithmic scale the anodic current transients experimentally obtained at potential jumps of 0.02 $V_{Li/Li+}$ to various lithium extraction potentials. All the anodic current transients showed two inflexion points, i.e. two quasi-current plateaux, throughout the whole lithium deintercalation. This

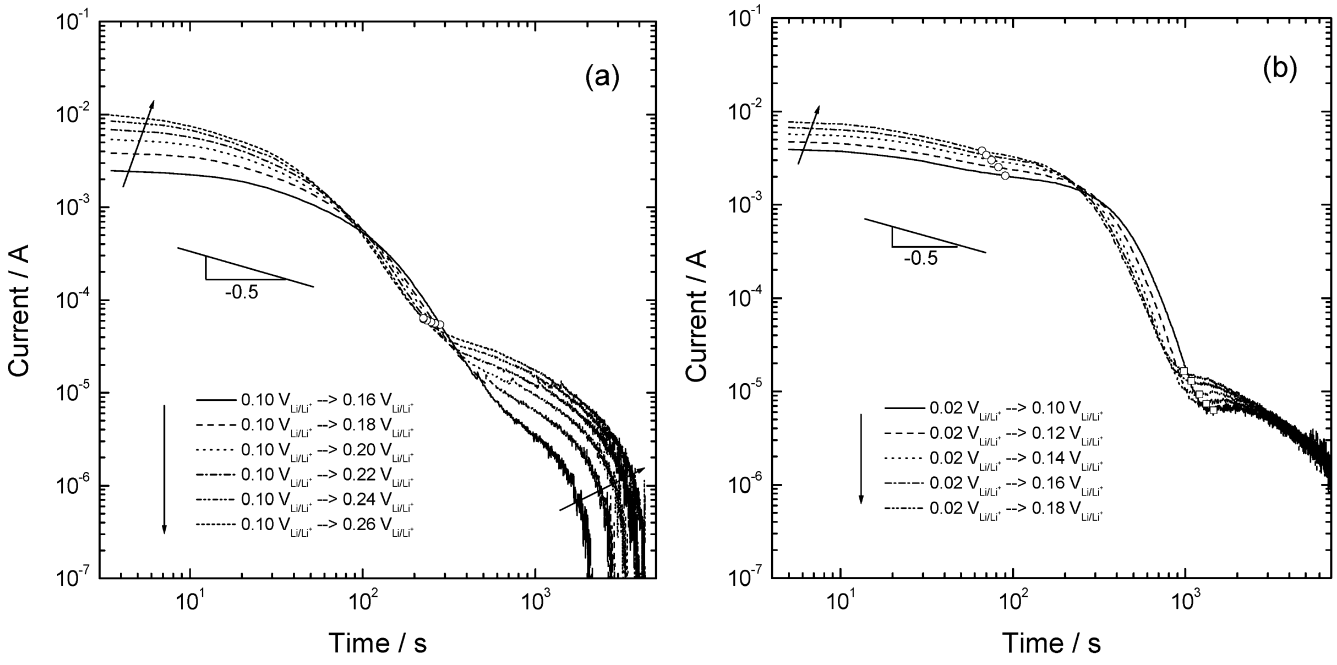

Fig. 5 The anodic current transients experimentally obtained from the Carbotron-P hard carbon composite electrode in a 1 M $LiPF_6$-EC/DEC solution at potential jumps of **a** 0.10 and **b** 0.02 $V_{Li/Li+}$ to various lithium extraction potentials as indicated in figure

means that, at this potential region, lithium ions can be deintercalated from the three different kinds of deintercalation sites with clearly distinguishable activation energies. Considering the activation energies for lithium deintercalation from the respective sites, it is most probable that the first inflexion point is caused by lithium deintercalation from both the sites for type III and type II, and the second inflexion point is due to lithium deintercalation from both the sites for type II and type IV.

In conclusion, from the good coincidence between the anodic current transients experimentally measured and theoretically calculated, it is strongly suggested that lithium transport through the Carbotron-P hard carbon composite electrode is governed by cell impedance, and at the same time the difference in activation energies for lithium deintercalation from the four different lithium deintercalation sites existing within the electrode is responsible for the different kinetics of lithium transport through the four different lithium deintercalation sites, which leads to the presence of the inflexion points, i.e. quasi-current plateaux, in the current transients.

Acknowledgements The receipt of a research grant under the internal research programme Technological Development of a High Performance Lithium Battery from the Korea Advanced Institute of Science and Technology (KAIST) 2000/2002 is gratefully acknowledged. This work was partly supported by the Brain Korea 21 project.

References

1. Funabiki A, Inaba M, Abe T, Ogumi Z (1999) J Electrochem Soc 146:2443
2. Funabiki A, Inaba M, Abe T, Ogumi Z (1999) Electrochim Acta 45:865
3. Wang C, Kakwan I, Appleby AJ, Little FE (2000) J Electroanal Chem 489:55
4. Shin HC, Pyun SI (1999) Electrochim Acta 45:489
5. Shin HC, Pyun SI, Kim SW, Lee MH (2001) Electrochim Acta 46:897
6. Pyun SI, Kim SW (2001) J Power Sources 97–98:371
7. Lee MH, Pyun SI, Shin HC (2001) Solid State Ionics 140:35
8. Pyun SI, Kim SW, Shin HC (1999) J Power Sources 81–82:248
9. Pyun SI, Lee SB, Chang WY (2002) J New Mater Electrochem Syst 5:281
10. Lee SB, Pyun SI (2002) Electrochim Acta 48:419
11. Lee SB, Pyun SI (2002) J Solid State Electrochem (in press)
12. Sato K, Noguchi M, Demachi A, Oki N, Endo M (1994) Science 264:556
13. Yata S, Kinoshita H, Komori M, Ando N, Kashiwamura T, Harada T, Tanaka K, Yamabe T (1994) Synth Met 62:153
14. Peled E, Menachem C, Bar-Tow D, Melman A (1996) J Electrochem Soc 143:L4
15. Tokumitsu K, Mabuchi A, Fujimoto H, Kasuh T (1996) J Electrochem Soc 143:2235
16. Mochida I, Ku CH, Korai Y (2001) Carbon 39:399
17. Shin HC, Pyun SI (2002) In: White RE, Conway BE, Vayenas CG (eds) Modern aspects of electrochemistry, vol 36. Plenum Press, New York, pp 255–301
18. Bard AJ, Faulkner LR (1980) Electrochemical methods. Wiley, New York, pp 136–212
19. McNabb A, Foster PK (1963) Trans Met Soc AIME 227:618
20. Pyun SI, Yang TH (1998) J Electroanal Chem 441:183
21. Weppner W, Huggins RA (1977) J Electrochem Soc 124:1569
22. Shewmon P (1989) Diffusion in solids. TMS, Pennsylvania, pp 53–96
23. Van der Ven A, Ceder G (2000) Electrochem Solid State Lett 3:301